J. Math. Anal. Appl. 410 (2014) 275–291

Contents lists available at ScienceDirect

Journal of Mathematical Analysis and Applications

www.elsevier.com/locate/jmaa

# Analysis of the convected Helmholtz equation with a uniform mean flow in a waveguide with complete radiation boundary conditions

Seungil Kim

*Department of Mathematics and Research Institute for Basic Sciences, Kyung Hee University, Seoul 130-701, Republic of Korea*

ARTICLE INFO

*Article history:*
Received 2 July 2012
Available online 21 August 2013
Submitted by W.L. Wendland

*Keywords:*
Waveguide
Helmholtz equation
Convected Helmholtz equation
Complete radiation boundary conditions
Prandtl–Glauert transformation

ABSTRACT

In this paper, we propose complete radiation boundary conditions (CRBCs) for solutions of the convected Helmholtz equation with a uniform mean flow in a waveguide. We first study CRBCs for the Helmholtz equation in a waveguide. Noting that the convected Helmholtz equation is associated with the Helmholtz equation via the Prandtl–Glauert transformation, CRBCs for the convected Helmholtz equation is derived from CRBCs for the Helmholtz equation. We analyse well-posedness and convergence of approximate solutions satisfying CRBCs for the convected Helmholtz equation. In addition, simple numerical experiments will be presented to confirm the theoretical results.

© 2013 Elsevier Inc. All rights reserved.

## 1. Introduction

In this paper, we consider an application of complete radiation boundary conditions (CRBCs) to a time-harmonic wave propagation problem in an unbounded waveguide with a uniform mean flow. Since numerical simulations for wave propagation problems require a domain truncation procedure without producing any reflection, there has been intensive research on developing non-reflecting boundary conditions such as methods based on Dirichlet-to-Neumann operators [8,16], perfectly matched layer (PML) techniques [4,5] and a high-order absorbing boundary conditions (ABCs) [7,12,13] including CRBCs [14,15]. For the general review of this subject, see e.g. [6,10,20].

The original CRBCs were proposed to solve wave propagation problems in the time-domain [14,15]. For time-domain calculations, CRBCs employ recursive formulations involving auxiliary functions, which avoid higher-order derivatives in Higdon's product boundary operators [17,18]. Thus, these boundary conditions can be naturally implemented in discrete techniques such as the finite element method or finite difference method. Theoretical and experimental results can be found in a variety of situations including first-order hyperbolic equations [14], second-order forms [15] and convected wave equations [11].

This paper is devoted to developing a local high-order ABCs for the convected Helmholtz equation in waveguides. In [19], well-posedness and convergence analysis of CRBCs applied to the Helmholtz equation in waveguides are investigated. We do this for the case in presence of a uniform mean flow. An interesting phenomenon of wave propagations in a uniform mean flow is that a solution may have modes whose direction in group velocity is different from that of phase velocity. When this is the case, it is important to identify correct radiating solutions, which plays a crucial role in developing non-reflecting boundary conditions on fictitious boundaries. The convected Helmholtz equations in ducts using PML have been studied in [2]. There, to avoid instability of upstream modes in the framework of standard PML, Bécache et al. in [2] examine

*E-mail address:* sikim@khu.ac.kr.

0022-247X/$ – see front matter © 2013 Elsevier Inc. All rights reserved.
http://dx.doi.org/10.1016/j.jmaa.2013.08.018

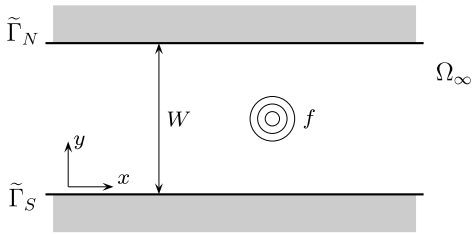



**Fig. 1.** Geometry of an infinite waveguide $\Omega_\infty$, $\widetilde{\Gamma}_T = \widetilde{\Gamma}_N \cup \widetilde{\Gamma}_S$.

the distribution of axial wavenumbers and introduce a new PML technique involving a translation together with standard complex coordinate stretchings of PML.

The main idea of developing CRBCs for the convected Helmholtz equation is related with the new PML approach. But here we will interpret modified CRBCs in terms of so-called the Prandtl–Glauert transformation (or Lorentz transformation) in aerodynamic context, by which the convected Helmholtz equation can be associated to the Helmholtz equation. Noticing that radiating solutions in the convected Helmholtz equations correspond to the counterparts in the Helmholtz equation via the Prandtl–Glauert transformation, our strategy is that we first develop CRBCs for the Helmholtz equation and then revert them back to the problem in the moving medium.

It is worth pointing out that CRBCs have many preferable properties as mentioned in [19]. CRBCs can be designed to control both propagating modes and evanescent modes and make a desirable performance even if wave sources are quite close to the absorbing boundaries. In addition, an advantage of CRBCs over ABCs based on DtN operators [3,9,16] is that CRBCs are local boundary conditions and do not need the knowledge of eigenvalues of the transverse Laplace operator on the cross-section of waveguides. Related to the distribution of transversal eigenvalues, there is an important issue on the optimal parameters of CRBCs. This issue for a general situation was discussed in [14] for time-domain problems and [19] for frequency-domain problems. When an information on the distribution of the eigenvalues are available, the efficiency of CRBCs can be improved by taking the optimal parameters determined by the axial wavenumbers, with which CRBCs annihilate modes associated with the corresponding axial wavenumbers. This fact will be illustrated in the numerical examples later.

Following is the outline of the remaining paper. Section 2 describes the problem in case of no flow and defines CRBCs for the Helmholtz equation with sources in waveguides. Here well-posedness and convergence analysis will be done. In Section 3, we consider the convected Helmholtz equation with a uniform mean flow. Identifying the radiating solutions and using the Prandtl–Glauert transformation, we will derive CRBCs for the convected Helmholtz equation. Using the results analyzed in Section 2, we prove the well-posedness and convergence of approximate solutions to the convected Helmholtz equation satisfying CRBCs as order of CRBCs increases. In Section 4, numerical experiments will be presented to demonstrate the theoretical results.

## 2. Complete radiation boundary conditions for the Helmholtz equation with sources in waveguides

In this section, we are concerned with a time-harmonic wave propagation problem in a medium with no flow in $\Omega_\infty$, where $\Omega_\infty$ is two dimensional infinite waveguide parallel to the $x$-axis of the Cartesian coordinates and has the width $W$, i.e., $\Omega_\infty = \mathbb{R} \times I_y$ with $I_y = (0, W)$ (see Fig. 1). Under the time-harmonic assumption with the time dependency $e^{-i\omega t}$, $\omega > 0$ angular frequency, and sound-hard boundary conditions on the waveguide, the acoustic pressure field $u_{ex}$ satisfies the Helmholtz equation with wavenumber $k = \omega/c_0$ ($c_0$ is sound speed in the medium):

$$\begin{aligned} &\Delta u_{ex} + k^2 u_{ex} = f \quad \text{in } \Omega_\infty, \\ &\frac{\partial u_{ex}}{\partial n} = 0 \quad \text{on } \widetilde{\Gamma}_T, \end{aligned} \tag{2.1}$$

with a radiation condition at infinity, where $f$ is a wave source supported on $|x| < L$ with a constant $L > 0$ and $n$ is the outward unit normal vector on $\widetilde{\Gamma}_T$. By introducing the modal basis functions of the 1-dimensional transverse Laplacian, associated with eigenvalues $\lambda_n^2 = (n\pi/W)^2$,

$$Y_0(y) = \sqrt{\frac{1}{W}}, \qquad Y_n(y) = \sqrt{\frac{2}{W}} \cos\left(\frac{n\pi}{W} y\right) \quad \text{for } n = 1, 2, \ldots$$

solving

$$-Y_n''(y) = \lambda_n^2 Y_n(y)$$

with $Y_n'(0) = Y_n'(W) = 0$, the radiating solution $u_{ex}$ has a series representation

$$u_{ex}(x, y) = \begin{cases} \sum_{n=0}^{\infty} A_n^E e^{i\mu_n x} Y_n(y) & \text{for } x > L, \\ \sum_{n=0}^{\infty} A_n^W e^{-i\mu_n x} Y_n(y) & \text{for } x < -L, \end{cases} \tag{2.2}$$

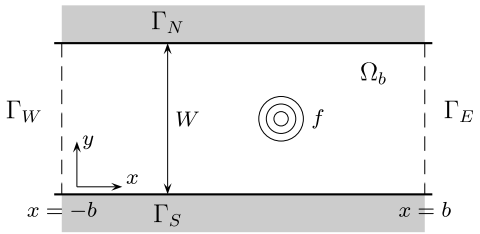



**Fig. 2.** Geometry of the truncated domain $\Omega_b$, $\Gamma_T = \Gamma_N \cup \Gamma_S$.

where $\mu_n^2 = k^2 - \lambda_n^2$. There are only finitely many $\mu_n^2 > 0$, for which positive axial wavenumber $\mu_n > 0$ is chosen and so they are associated with propagating modes. On the other hands, there are infinitely many $\mu_n^2 < 0$ and we take $\mu_n$ with $\tilde{\mu}_n \equiv \Im(\mu_n) > 0$ and so the modes corresponding to the axial wavenumber decay exponentially. Lastly, there may be a situation when $\mu_n^2 = 0$. In such a case, since a solution to the problem is not unique, from here on we assume that $\mu_n^2 \neq 0$.

When the problem is reduced to a problem posed in a finite computational domain $\Omega_b = (-b, b) \times I_y$ with $b > L$ (see Fig. 2), the radiating condition at infinity needs to be replaced with absorbing boundary conditions on $\Gamma_E \cup \Gamma_W$. For this, complete radiation boundary conditions will be enforced on the artificial boundaries.

### 2.1. Complete radiation boundary conditions on $\Gamma_E$

Denote an interval $(L, b)$ by $I_E$ and define

$$\mathcal{H}_E = \left\{ v \in H^1(I_E \times I_y) \colon \Delta v + k^2 v = 0 \text{ in } I_E \times I_y \text{ with } \frac{\partial v}{\partial n} = 0 \text{ on } I_E \times \partial I_y \text{ and } v|_{\Gamma_E} \in H^1(\Gamma_E) \right\}. \tag{2.3}$$

Here $H^1$ spaces are standard Sobolev spaces of functions that are $L^2$ integrable together with their first derivatives in some prescribed domains. For CRBCs on $\Gamma_E$, we introduce auxiliary functions $\phi_j^E$ in $\mathcal{H}_E$ satisfying the recursive formulas in $I_E \times I_y$

$$\begin{aligned} &\phi_0^E = u, \\ &\left(\frac{\partial}{\partial x} + a_j\right)\phi_j^E = \left(-\frac{\partial}{\partial x} + a_j\right)\phi_{j+1}^E \end{aligned} \tag{2.4}$$

for $j = 0, 1, 2, \ldots$, where $a_j$ are parameters to be chosen for reducing reflection from the artificial boundary. This recursion is terminated by

$$\phi_{p+1}^E = 0 \quad \text{on } x = b. \tag{2.5}$$

In other words, if we introduce a linear operator $B_p^E : \mathcal{H}_E \to H^1(\Gamma_E)$ defining $B_p^E(u)$ by the restriction of $\phi_{p+1}^E$ on $\Gamma_E$ for $u \in \mathcal{H}_E$, then the CRBCs on $\Gamma_E$ is the boundary condition

$$B_p^E(u) = 0 \quad \text{on } \Gamma_E. \tag{2.6}$$

For the damping parameters $a_j$, two different types of $a_j$ are considered in [19]. The first approach is to choose $a_j$ in a way that each term in (2.4) damps reflection of propagating modes and evanescent modes simultaneously. For this purpose, we choose

$$a_j = \sigma_j - ikc_j \tag{2.7}$$

with

$$\epsilon < \sigma_j < 1/\epsilon \quad \text{and} \quad \epsilon < c_j \leqslant 1 \tag{2.8}$$

for some positive $\epsilon$. We note that the direct application of the time-domain parameters derived in [14] would lead to

$$c_j = \cos(\theta_j), \qquad \sigma_j = \frac{1 - c_j^2}{\eta c_j}. \tag{2.9}$$

Here $\eta$ is a limiting absorption parameter and $\theta_j$ signify angles of incident waves in $(0, \frac{\pi}{2})$. The second approach is to choose $a_j$ for which the right differential operators of (2.4) annihilate Fourier modes corresponding to a certain axial wavenumber, that is, we choose

$$a_j = \begin{cases} -ikc_j & \text{for } j = 0, \ldots, n_p - 1, \\ \sigma_{j-n_p} & \text{for } j = n_p, \ldots, n_p + n_e \end{cases} \tag{2.10}$$

with the same conditions on $\sigma_j$ and $c_j$ as above. Among the two approaches, for simple presentation, we only consider CRBCs employing parameters $a_j$ defined by (2.7). The analysis for the other case of $a_j$ can be carried out by following the same idea with a small modification as can be seen in [19].

In order to derive boundary conditions suitable for numerical computations, all normal derivatives in the recursions need to be eliminated. We do this by simple algebraic computations as in [19] and see that

$$2\frac{\partial u}{\partial x} = L_{0,0}\frac{\partial^2\phi_0^E}{\partial y^2} + L_{0,1}\frac{\partial^2\phi_1^E}{\partial y^2} + k^2\big(L_{0,0}\phi_0^E + L_{0,1}\phi_1^E\big) - \big(M_{0,0}\phi_0^E + M_{0,1}\phi_1^E\big), \tag{2.11}$$

$$\begin{aligned} 0 = {} & L_{j,j-1}\frac{\partial^2\phi_{j-1}^E}{\partial y^2} + L_{j,j}\frac{\partial^2\phi_j^E}{\partial y^2} + L_{j,j+1}\frac{\partial^2\phi_{j+1}^E}{\partial y^2} + k^2\big(L_{j,j-1}\phi_{j-1}^E + L_{j,j}\phi_j^E + L_{j,j+1}\phi_{j+1}^E\big) \\ & - \big(M_{j,j-1}\phi_{j-1}^E + M_{j,j}\phi_j^E + M_{j,j+1}\phi_{j+1}^E\big) \end{aligned} \tag{2.12}$$

for $j = 1, \ldots, p$, where

$$L_{0,0} = \frac{1}{a_0}, \qquad L_{0,1} = L_{1,0} \quad \text{and} \quad M_{0,0} = a_0, \qquad M_{0,1} = M_{1,0}$$

and for $j = 1, \ldots, p$

$$\begin{aligned} & L_{j,j-1} = \frac{1}{a_{j-1}}, \qquad L_{j,j} = \frac{1}{a_{j-1}} + \frac{1}{a_j}, \qquad L_{j,j+1} = \frac{1}{a_j}, \\ & M_{j,j-1} = -a_{j-1}, \qquad M_{j,j} = a_{j-1} + a_j, \qquad M_{j,j+1} = -a_j. \end{aligned}$$

By taking (2.5) into account, combining (2.11) and (2.12) gives the boundary condition involving $(p+1)\times(p+1)$ symmetric tridiagonal matrices $L$ and $M$,

$$\left(\frac{\partial u}{\partial x}\right)\boldsymbol{e}_0 = \frac{1}{2}\left(L\frac{\partial^2\Phi^E}{\partial y^2} + \big(k^2L - M\big)\Phi^E\right),$$

where $\boldsymbol{e}_0$ is the standard $(p+1)\times 1$ basis vector whose non-zero element is one at the zeroth component and $\Phi^E = (\phi_0^E, \ldots, \phi_p^E)^t$.

### 2.2. Complete radiation boundary conditions on $\Gamma_W$

The CRBCs on $\Gamma_W$ is defined analogously. Denoting $I_W = (-b, -L)$, let us define

$$\mathcal{H}_W = \left\{ v \in H^1(I_W \times I_y) \colon \Delta v + k^2 v = 0 \text{ in } I_W \times I_y \text{ with } \frac{\partial v}{\partial n} = 0 \text{ on } I_W \times \partial I_y \text{ and } v|_{\Gamma_W} \in H^1(\Gamma_W) \right\}. \tag{2.13}$$

As above, using a sequence of functions $\phi_j^W \in \mathcal{H}_W$ satisfying

$$\begin{aligned} & \phi_0^W = u, \\ & \left(-\frac{\partial}{\partial x} + a_j\right)\phi_j^W = \left(\frac{\partial}{\partial x} + a_j\right)\phi_{j+1}^W \end{aligned} \tag{2.14}$$

in $I_W \times I_y$ for $j = 0, 1, \ldots$, we introduce a linear operator $B_p^W : \mathcal{H}_W \to H^1(\Gamma_W)$ defining $B_p^W(u)$ by the restriction of $\phi_{p+1}^W$ on $\Gamma_W$. Then the CRBCs on $\Gamma_W$ is the boundary condition

$$B_p^W(u) = 0 \quad \text{on } \Gamma_W \tag{2.15}$$

for $u \in \mathcal{H}^W$. Also, we can derive practical boundary conditions by eliminating all normal derivatives from the recursions (2.14) as in the case for CRBCs on $\Gamma_E$ and we have

$$\left(\frac{\partial u}{\partial x}\right)\boldsymbol{e}_0 = \frac{-1}{2}\left(L\frac{\partial^2\Phi^W}{\partial y^2} + \big(k^2L - M\big)\Phi^W\right),$$

where $\Phi^W = (\phi_0^W, \ldots, \phi_p^W)^t$.

### 2.3. Well-posedness

We first introduce the following Sobolev spaces. Let us define

$$\widetilde{H}^1(\Omega_b) = \{\xi \in H^1(\Omega_b): \xi|_{\Gamma_E} \in H^1(\Gamma_E) \text{ and } \xi|_{\Gamma_W} \in H^1(\Gamma_W)\}.$$

The solution space $\boldsymbol{H}$ is defined by

$$\boldsymbol{H} = \{(u, \Phi^E, \Phi^W) \in \widetilde{H}^1(\Omega_b) \times (H^1(\Gamma_E))^{p+1} \times (H^1(\Gamma_W))^{p+1}: u = \phi_0^E \text{ on } \Gamma_E \text{ and } u = \phi_0^W \text{ on } \Gamma_W\}$$

equipped with the Sobolev norm

$$\|(u, \Phi^E, \Phi^W)\|_{\boldsymbol{H}}^2 = \|u\|_{H^1(\Omega_b)}^2 + \|\Phi^E\|_{\boldsymbol{H}^1(\Gamma_E)}^2 + \|\Phi^W\|_{\boldsymbol{H}^1(\Gamma_W)}^2,$$

where

$$\|\Phi^*\|_{\boldsymbol{H}^1(\Gamma_*)}^2 = \sum_{j=0}^{p} \|\phi_j^* + \phi_{j+1}^*\|_{H^1(\Gamma_*)}^2$$

with $\phi_{p+1}^* = 0$. In the above definition, $*$ represents $E$ or $W$. Noting that the norm $\|\cdot\|_{\boldsymbol{H}^1(\Gamma_*)}$ is equivalent to the standard product norm

$$\|\Phi^*\|_{(H^1(\Gamma_*))^{p+1}}^2 = \sum_{j=0}^{p} \|\phi_j^*\|_{H^1(\Gamma_*)}^2,$$

we observe that $\boldsymbol{H}$ is closed in $H^1(\Omega_b) \times (H^1(\Gamma_E))^{p+1} \times (H^1(\Gamma_W))^{p+1}$ and hence is a Hilbert space. Also, we will use a subspace $\boldsymbol{L}^2$ of $L^2(\Omega_b) \times (L^2(\Gamma_E))^{p+1} \times (L^2(\Gamma_W))^{p+1}$

$$\boldsymbol{L}^2 = \{(u, \Phi^E, \Phi^W) \in L^2(\Omega_b) \times (L^2(\Gamma_E))^{p+1} \times (L^2(\Gamma_W))^{p+1}: u = \phi_0^E \text{ on } \Gamma_E \text{ and } u = \phi_0^W \text{ on } \Gamma_W\}$$

having a norm

$$\|(u, \Phi^E, \Phi^W)\|_{\boldsymbol{L}^2}^2 = \|u\|_{L^2(\Omega_b)}^2 + \|\Phi^E\|_{\boldsymbol{L}^2(\Gamma_E)}^2 + \|\Phi^W\|_{\boldsymbol{L}^2(\Gamma_W)}^2$$

with

$$\|\Phi^*\|_{\boldsymbol{L}^2(\Gamma_*)}^2 = \sum_{j=0}^{p} \|\phi_j^* + \phi_{j+1}^*\|_{L^2(\Gamma_*)}^2.$$

Now, we will seek for a solution $(u, \Phi^E, \Phi^W) \in \boldsymbol{H}$ solving

$$\Delta u + k^2 u = f \quad \text{in } \Omega_b, \tag{2.16}$$

$$\frac{\partial u}{\partial n} = 0 \quad \text{on } \Gamma_T, \tag{2.17}$$

$$\left(\frac{\partial u}{\partial x}\right)\boldsymbol{e}_0 = \frac{1}{2}\left(L\frac{\mathrm{d}^2\Phi^E}{\mathrm{d}y^2} + (k^2 L - M)\Phi^E\right) \quad \text{on } \Gamma_E, \tag{2.18}$$

$$\left(\frac{\partial u}{\partial x}\right)\boldsymbol{e}_0 = \frac{-1}{2}\left(L\frac{\mathrm{d}^2\Phi^W}{\mathrm{d}y^2} + (k^2 L - M)\Phi^W\right) \quad \text{on } \Gamma_W \tag{2.19}$$

with $\mathrm{d}\Phi^E/\mathrm{d}y = 0$ on $\partial\Gamma_E$ and $\mathrm{d}\Phi^W/\mathrm{d}y = 0$ on $\partial\Gamma_W$.

**Lemma 2.1.** *A solution $(u, \Phi^E, \Phi^W) \in \boldsymbol{H}$ to the problem (2.16)–(2.19) is unique.*

**Proof.** Assume that $f = 0$. Now, we can expand all components of the solution $(u, \Phi^E, \Phi^W)$ in terms of modal basis functions $Y_n$,

$$u(x, y) = \sum_{n=0}^{\infty} (A_n^+ e^{i\mu_n x} + A_n^- e^{-i\mu_n x}) Y_n(y),$$

$$\phi_j^E(y) = \sum_{n=0}^{\infty} E_j^n Y_n(y) \quad \text{and} \quad \phi_j^W(y) = \sum_{n=0}^{\infty} W_j^n Y_n(y).$$

By $\boldsymbol{E}^n$ and $\boldsymbol{W}^n$ denote $(p+1)\times 1$ vectors whose components consists of the $n$-th Fourier coefficients of $\Phi^E$ and $\Phi^W$, respectively. Examining the $n$-th Fourier modes from (2.18) and (2.19), we are led to

$$2i\mu_n\big(A_n^+e^{i\mu_n b}-A_n^-e^{-i\mu_n b}\big)\boldsymbol{e}_0=\mu_n^2L\boldsymbol{E}^n-M\boldsymbol{E}^n, \tag{2.20}$$

$$2i\mu_n\big(A_n^+e^{-i\mu_n b}-A_n^-e^{i\mu_n b}\big)\boldsymbol{e}_0=-\mu_n^2L\boldsymbol{W}^n+M\boldsymbol{W}^n. \tag{2.21}$$

Noting that $E_0^n=A_n^+e^{i\mu_n b}+A_n^-e^{-i\mu_n b}$, the inner-product of (2.20) against $\boldsymbol{E}^n$ in $\mathbb{C}^{p+1}$ shows that from the left hand side

$$\begin{aligned}LHS_E&=2i\mu_n\big(A_n^+e^{i\mu_n b}-A_n^-e^{-i\mu_n b}\big)\bar{E}_0^n\\&=\begin{cases}-4\mu_n\Im(A_n^+\bar{A}_n^-e^{2i\mu_n b})+2\mu_n(|A_n^+|^2-|A_n^-|^2)i & \text{if } \mu_n^2>0,\\ -2\tilde{\mu}_n(|A_n^+|^2e^{-2\tilde{\mu}_n b}-|A_n^-|^2e^{2\tilde{\mu}_n b})-4\tilde{\mu}_n\Im(A_n^+\bar{A}_n^-)i & \text{if } \mu_n^2<0\end{cases}\end{aligned} \tag{2.22}$$

and from the right hand side

$$\begin{aligned}RHS_E&=\mu_n^2\big(L\boldsymbol{E}^n,\boldsymbol{E}^n\big)_{\mathbb{C}^{p+1}}-\big(M\boldsymbol{E}^n,\boldsymbol{E}^n\big)_{\mathbb{C}^{p+1}}\\&=\sum_{j=0}^{p}\left[\frac{\mu_n^2}{a_j}\big|E_j^n+E_{j+1}^n\big|^2-a_j\big|E_j^n-E_{j+1}^n\big|^2\right],\end{aligned} \tag{2.23}$$

where $E_{p+1}^n=0$ and $\bar{\cdot}$ stands for the complex conjugate of $\cdot$. Similarly, using (2.21) and $W_0^n=A_n^+e^{-i\mu_n b}+A_n^-e^{i\mu_n b}$, we find out that from the left hand side

$$\begin{aligned}LHS_W&=2i\mu_n\big(A_n^+e^{-i\mu_n b}-A_n^-e^{i\mu_n b}\big)\bar{W}_0^n\\&=\begin{cases}-4\mu_n\Im(A_n^+\bar{A}_n^-e^{-2i\mu_n b})+2\mu_n(|A_n^+|^2-|A_n^-|^2)i & \text{if } \mu_n^2>0,\\ -2\tilde{\mu}_n(|A_n^+|^2e^{2\tilde{\mu}_n b}-|A_n^-|^2e^{-2\tilde{\mu}_n b})-4\tilde{\mu}_n\Im(A_n^+\bar{A}_n^-)i & \text{if } \mu_n^2<0\end{cases}\end{aligned} \tag{2.24}$$

and from the right hand side

$$\begin{aligned}RHS_W&=\mu_n^2\big(L\boldsymbol{W}^n,\boldsymbol{W}^n\big)_{\mathbb{C}^{p+1}}-\big(M\boldsymbol{W}^n,\boldsymbol{W}^n\big)_{\mathbb{C}^{p+1}}\\&=\sum_{j=0}^{p}\left[\frac{-\mu_n^2}{a_j}\big|W_j^n+W_{j+1}^n\big|^2+a_j\big|W_j^n-W_{j+1}^n\big|^2\right]\end{aligned} \tag{2.25}$$

with $W_{p+1}^n=0$.

Now, we shall show that all Fourier coefficients, $A_n^+$, $A_n^-$, $E_n^j$ and $W_n^j$ vanish for both cases $\mu_n^2>0$ and $\mu_n^2<0$. When $\mu_n^2>0$, comparing the imaginary parts of (2.22) and (2.23) yields that

$$2\mu_n\big(\big|A_n^+\big|^2-\big|A_n^-\big|^2\big)=\sum_{j=0}^{p}\left[\Im\left(\frac{\mu_n^2}{a_j}\right)\big|E_j^n+E_{j+1}^n\big|^2-\Im(a_j)\big|E_j^n-E_{j+1}^n\big|^2\right]. \tag{2.26}$$

Since $\Im(\mu_n^2/a_j)$ and $-\Im(a_j)$ are all positive, it then follows that

$$\big|A_n^+\big|^2-\big|A_n^-\big|^2\geqslant 0. \tag{2.27}$$

On the other hands, the same argument used above can be applied to the imaginary parts of (2.24) and (2.25) and results in

$$\big|A_n^+\big|^2-\big|A_n^-\big|^2\leqslant 0. \tag{2.28}$$

Therefore, (2.27) and (2.28) shows that $|A_n^+|=|A_n^-|$, which in turn implies that $E_j^n=W_j^n=0$ for $j=0,\dots,p$ from (2.26) and its analogous part for $\boldsymbol{W}^n$. In addition, since $E_0^n=E_1^n=0$, by reading the zeroth row of (2.18) we observe that the $n$-th Fourier coefficient of $\partial u/\partial x$ on $\Gamma_E$ vanishes, which implies

$$A_n^+e^{i\mu_n b}-A_n^-e^{-i\mu_n b}=0.$$

Also, since $u(b,\cdot)=\phi_0^E(\cdot)$, we have

$$A_n^+e^{i\mu_n b}+A_n^-e^{-i\mu_n b}=0.$$

Clearly, the above two equations have only trivial solution $A_n^+=A_n^-=0$.

Next, let us consider the case when $\mu_n^2<0$. In this case, we compare the real parts of (2.22) and (2.23),

$$-2\tilde{\mu}_n\left(\left|A_n^+\right|^2 e^{-2\tilde{\mu}_n b} - \left|A_n^-\right|^2 e^{2\tilde{\mu}_n b}\right) = \sum_{j=0}^{p}\left[\Re\left(\frac{\mu_n^2}{a_j}\right)\left|E_n^j + E_{j+1}^n\right|^2 - \Re(a_j)\left|E_n^j + E_n^{j+1}\right|^2\right], \tag{2.29}$$

and since $\tilde{\mu}_n > 0$, $\Re(\frac{\mu_n^2}{a_j}) < 0$ and $-\Re(a_j) < 0$, we obtain that

$$\left|A_n^+\right|^2 e^{-2\tilde{\mu}_n b} - \left|A_n^-\right|^2 e^{2\tilde{\mu}_n b} \geqslant 0. \tag{2.30}$$

Similarly, from (2.24) and (2.25), it follows that

$$\left|A_n^+\right|^2 e^{2\tilde{\mu}_n b} - \left|A_n^-\right|^2 e^{-2\tilde{\mu}_n b} \leqslant 0. \tag{2.31}$$

Examining (2.30) and (2.31) with the help of $\tilde{\mu}_n b > 0$, it can be concluded that $A_n^+ = A_n^- = 0$, which in turn proves $E_n^j = W_n^j = 0$ for $j = 0, \ldots, p$ from (2.29) and its analogous part for $\boldsymbol{W}_n$.

Finally, since $A_n^+ = A_n^- = 0$ and $E_n^j = W_n^j = 0$ for all $n \in \mathbb{N}$ and $j = 0, \ldots, p$, the solution $(u, \Phi^E, \Phi^W)$ is a trivial one, which completes the proof. □

**Remark 2.2.** This uniqueness result shows that the boundary conditions (2.6) ((2.15), respectively) involving the recursions (2.4) ((2.14), respectively) are equivalent to the boundary conditions (2.18) ((2.19), respectively). In fact, by construction of the boundary conditions (2.18) and (2.19), the solution satisfying the boundary conditions (2.6) and (2.15) fulfill the boundary condition (2.18) and (2.19). Conversely, the uniqueness lemma implies that only the solution satisfying (2.6) and (2.15) is one that meets the conditions (2.18) and (2.19).

Now, we take test functions $(\xi, \Psi^E, \Psi^W) \in \boldsymbol{H}$, multiply (2.16), (2.18) and (2.19) by $2\xi$, $\Psi^E$ and $\Psi^W$ respectively, and integrate them parts to obtain the weak problem to find $(u, \Phi^E, \Phi^W)$ in $\boldsymbol{H}$ such that

$$A\left(\left(u, \Phi^E, \Phi^W\right), \left(\xi, \Psi^E, \Psi^W\right)\right) = (2f, \xi)_{\Omega_b} \quad \text{for all } \left(\xi, \Psi^E, \Psi^W\right) \in \boldsymbol{H}, \tag{2.32}$$

where

$$\begin{aligned} A\left(\left(u, \Phi^E, \Phi^E\right), \left(\xi, \Psi^E, \Psi^W\right)\right) &= 2(\nabla u, \nabla \xi)_{\Omega_b} - 2k^2(u, \xi)_{\Omega_b} \\ &\quad + \left(L\frac{\mathrm{d}\Phi^E}{\mathrm{d}y}, \frac{\mathrm{d}\Psi^E}{\mathrm{d}y}\right)_{\Gamma_E} + \left(\left(-k^2 L + M\right)\Phi^E, \Psi^E\right)_{\Gamma_E} \\ &\quad + \left(L\frac{\mathrm{d}\Phi^W}{\mathrm{d}y}, \frac{\mathrm{d}\Psi^W}{\mathrm{d}y}\right)_{\Gamma_E} + \left(\left(-k^2 L + M\right)\Phi^E, \Psi^W\right)_{\Gamma_W}. \end{aligned}$$

Here we used $(\cdot,\cdot)_{\Omega_b}$ and $(\cdot,\cdot)_{\Gamma_*}$ for $L^2$ inner-product on $\Omega_b$ and $\Gamma_*$, respectively.

To establish well-posedness of the problem (2.32), we need the following lemmas.

**Lemma 2.3.** *Suppose that $\Theta = (\theta_0, \ldots, \theta_p)^t$ is a vector in $\mathbb{C}^{p+1}$. Then there exists a positive constant $C_L$ such that*

$$C_L \sum_{j=0}^{p} |\theta_j + \theta_{j+1}|^2 \leqslant \left|(L\Theta, \Theta)_{\mathbb{C}^{p+1}}\right|$$

*with $\theta_{p+1} = 0$.*

**Proof.** Since $\Re(\frac{1}{a_j}) > C_L > 0$ for a constant $C_L$, it is easy to show that

$$\Re\left((L\Theta, \Theta)_{\mathbb{C}^{p+1}}\right) = \sum_{j=0}^{p} \Re\left(\frac{1}{a_j}\right)|\theta_j + \theta_{j+1}|^2 \geqslant C_L \sum_{j=0}^{p} |\theta_j + \theta_{j+1}|^2,$$

which leads to the desired inequality. □

**Lemma 2.4.** *There exists a positive constant $C$ such that*

$$\left\|\left(u, \Phi^E, \Phi^W\right)\right\|_{\boldsymbol{H}} \leqslant C \sup_{(\xi, \Psi^E, \Psi^W) \in \boldsymbol{H}} \frac{\left|A\left(\left(u, \Phi^E, \Phi^W\right), \left(\xi, \Psi^E, \Psi^W\right)\right)\right|}{\left\|\left(\xi, \Psi^E, \Psi^W\right)\right\|_{\boldsymbol{H}}}$$

*and*

$$\left\|\left(u,\Phi^E,\Phi^W\right)\right\|_{\boldsymbol{H}} \leqslant C \sup_{(\xi,\Psi^E,\Psi^W)\in\boldsymbol{H}} \frac{|A((\xi,\Psi^E,\Psi^W),(u,\Phi^E,\Phi^W))|}{\|(\xi,\Psi^E,\Psi^W)\|_{\boldsymbol{H}}}$$

*for all* $(u,\Phi^E,\Phi^W)\in\boldsymbol{H}$.

**Proof.** We first show that there exist positive constants $J$ and $C$ such that

$$\left\|\left(u,\Phi^E,\Phi^W\right)\right\|_{\boldsymbol{H}}^2 \leqslant C\left|A\left(\left(u,\Phi^E,\Phi^W\right),\left(u,\Phi^E,\Phi^W\right)\right)+J\left\|\left(u,\Phi^E,\Phi^W\right)\right\|_{\boldsymbol{L}^2}^2\right|.$$

Indeed, noting that $\Re(a_j)>0$ and using Lemma 2.3, for any $J>0$

$$\begin{aligned}
&\Re\left(A\left(\left(u,\Phi^E,\Phi^W\right),\left(u,\Phi^E,\Phi^W\right)\right)+J\left\|\left(u,\Phi^E,\Phi^W\right)\right\|_{\boldsymbol{L}^2}^2\right)\\
&\quad\geqslant 2\|\nabla u\|_{L^2(\Omega_b)}^2+C_L\left\|\frac{\mathrm{d}\Phi^E}{\mathrm{d}y}\right\|_{\boldsymbol{L}^2(\Gamma_E)}^2+C_L\left\|\frac{\mathrm{d}\Phi^W}{\mathrm{d}y}\right\|_{\boldsymbol{L}^2(\Gamma_W)}^2+J\left\|\left(u,\Phi^E,\Phi^W\right)\right\|_{\boldsymbol{L}^2}^2\\
&\qquad-2k^2\|u\|_{L^2(\Omega_b)}^2-\max_{j=0}^{p}\left\{\frac{k^2}{|a_j|}\right\}\left(\left\|\Phi^E\right\|_{\boldsymbol{L}^2(\Gamma_E)}^2+\left\|\Phi^W\right\|_{\boldsymbol{L}^2(\Gamma_W)}^2\right).
\end{aligned}$$

By taking a sufficiently large $J>k^2\max\{2,1/|a_j|\}$, it is obtained that

$$\left|A\left(\left(u,\Phi^E,\Phi^W\right),\left(u,\Phi^E,\Phi^W\right)\right)+J\left\|\left(u,\Phi^E,\Phi^W\right)\right\|_{\boldsymbol{L}^2}^2\right|\geqslant C\left\|\left(u,\Phi^E,\Phi^W\right)\right\|_{\boldsymbol{H}}^2.$$

Finally, since the sesquilinear form $A(\cdot,\cdot)$ is bounded, due to the uniqueness of solutions in Lemma 2.1 and compact embedding of $\boldsymbol{H}$ into $\boldsymbol{L}^2$, the Fredholm alternative theorem completes the proof. □

The well-posedness of the variational problem (2.32) is an immediate result of Lemma 2.4.

**Theorem 2.5.** *For* $f\in L^2(\Omega_b)$ *supported in* $|x|<L$, *the problem* (2.32) *has a unique solution* $(u,\Phi^E,\Phi^W)\in\boldsymbol{H}$ *such that*

$$\left\|\left(u,\Phi^E,\Phi^W\right)\right\|_{\boldsymbol{H}}\leqslant C\|f\|_{L^2(\Omega_b)}.$$

### 2.4. Convergence analysis

In this section, we will prove the convergence of approximate solutions satisfying CRBCs of order $p$ as $p$ tends toward infinity.

**Theorem 2.6.** *Suppose that* $u_{ex}$ *is the radiating solution to the problem* (2.1) *for* $f\in L^2(\Omega_b)$ *supported in* $|x|<L$. *If* $(u,\Phi^E,\Phi^W)\in\boldsymbol{H}$ *is an approximate solution to the problem* (2.32), *then for any* $\varepsilon>0$ *there exist a positive constant and* $M(\varepsilon,u_{ex})<1$ *such that*

$$\|u_{ex}-u\|_{H^1(\Omega_b)}\leqslant C\left(M^{2(p+1)}+\varepsilon\right)\|u_{ex}\|_{H^1(\Omega_b)}, \tag{2.33}$$

*where* $C$ *is independent of* $\varepsilon$, $u$, $u_{ex}$ *and* $p$.

We know that Lemma 2.4 leads to well-posedness of the problem (2.32) for a fixed order $p$ of CRBCs, however the stability constant $C$ is not known to be free from $p$. Thus convergence analysis of approximate solutions needs to be approached rather than using Lemma 2.4. To do this, we first note that one can show the well-known result of well-posedness of the Helmholtz equation with the DtN operator by using the Fredholm alternative theorem.

**Lemma 2.7.** *Let* $T^*: H^{1/2}(\Gamma_*)\to H^{-1/2}(\Gamma_*)$ *be the Dirichlet-to-Neumann operator defined by*

$$T^*(w)=\sum_{n=0}^{\infty} i\mu_n(w,Y_n)_{\Gamma_*}Y_n, \tag{2.34}$$

*where* $*$ *represents* $E$ *or* $W$. *Then the sesquilinear form*

$$a(u,v)=(\nabla u,\nabla v)_{\Omega_b}-k^2(u,v)_{\Omega_b}-\left\langle T^E u,v\right\rangle_{\Gamma_E}-\left\langle T^W u,v\right\rangle_{\Gamma_W}$$

*satisfies an inf–sup condition*: *for* $u\in H^1(\Omega_b)$

$$\|u\|_{H^1(\Omega_b)}\leqslant C\sup_{v\in H^1(\Omega_b)}\frac{|a(u,v)|}{\|v\|_{H^1(\Omega_b)}}, \tag{2.35}$$

*with* $C$ *independent of* $u\in H^1(\Omega_b)$.

Here $H^s(\Gamma_*)$ is the Sobolev space equipped with the norm

$$\|\chi\|^2_{H^s(\Gamma_*)} = \sum_{n=0}^{\infty} (1+\lambda_n^2)^s |\chi_n|^2 < \infty,$$

where $\chi_n$ is Fourier coefficients of $\chi$. Also, $\langle\cdot,\cdot\rangle_{\Gamma_*}$ denotes the duality pairing between $H^{-1/2}(\Gamma_*)$ and $H^{1/2}(\Gamma_*)$.

Now, it is obvious that $u_{ex}$ solves the equation

$$a(u_{ex},\xi) = (f,\xi)_{\Omega_b} \quad \text{for all } \xi \in H^1(\Omega_b),$$

and then integration by parts shows that

$$a(u-u_{ex},\xi) = \left\langle T^E u - \frac{\partial u}{\partial x}, \xi \right\rangle_{\Gamma_E} + \left\langle T^W u + \frac{\partial u}{\partial x}, \xi \right\rangle_{\Gamma_W}.$$

For the convergence analysis, we begin with the inf–sup condition (2.35) for the error function $u-u_{ex}$,

$$\begin{aligned} \|u-u_{ex}\|_{H^1(\Omega_b)} &\leqslant C \sup_{\xi\in H^1(\Omega)} \frac{|a(u-u_{ex},\xi)|}{\|\xi\|_{H^1(\Omega_b)}} \\ &\leqslant C\left\| T^E(u) - \frac{\partial u}{\partial x}\right\|_{H^{-1/2}(\Gamma_E)} + \left\| T^W(u) + \frac{\partial u}{\partial x}\right\|_{H^{-1/2}(\Gamma_W)}. \end{aligned} \tag{2.36}$$

Thus, it suffices to estimate $\|T^E(u) - \partial u/\partial x\|_{H^{-1/2}(\Gamma_E)}$ (the analogous estimation on $\Gamma_W$ is identical): for any $\varepsilon > 0$, there exists a positive constant $M(\varepsilon, u_{ex}) < 1$ such that

$$\left\| T^E(u) - \frac{\partial u}{\partial x}\right\|_{H^{-1/2}(\Gamma_E)} \leqslant C\big(M^{2(p+1)} + \varepsilon\big)\|u_{ex}\|_{H^1(\Omega_b)}$$

with $C$ independent of $\varepsilon$, $u$, $u_{ex}$ and $p$.

As pointed out in [19], a radiating solution $u_{ex}$ to the Helmholtz equation (2.1) can be characterized in terms of complete radiation boundary conditions, that is, for the right-going behavior on the region of $x > L$ there exists a sequence of functions $\phi^E_{ex,j} \in \mathcal{H}_E$ satisfying the recursions (2.4) and the condition

$$\lim_{p\to\infty} \phi^E_{ex,p}(b,y) = 0. \tag{2.37}$$

Here, noting that $u_{ex}$ has the series expansions (2.2), the auxiliary functions can be written as

$$\phi^E_{ex,p}(x,y) = \sum_{n=0}^{\infty} \Pi_{p-1,n} A^E_n e^{i\mu_n x} Y_n(y), \tag{2.38}$$

where $\Pi_{p-1,n} = \prod_{j=0}^{p-1}(a_j + i\mu_n)/(a_j - i\mu_n)$. Similarly, the left-going behavior of the solution $u_{ex}$ in the region $x < -L$ can be interpreted by using a sequence of $\phi^W_{ex,j}$ in $\mathcal{H}_W$ satisfying the recursions (2.14) and the condition

$$\lim_{p\to\infty} \phi^W_{ex,p}(-b,y) = 0. \tag{2.39}$$

Also, the auxiliary functions have the following series representation

$$\phi^W_{ex,p}(x,y) = \sum_{n=0}^{\infty} \Pi_{p-1,n} A^W_n e^{-i\mu_n x} Y_n(y).$$

Then the error function $z = u - u_{ex}$ satisfies the boundary condition on $\Gamma_*$

$$B^*_p(z) = -\sum_{n=0}^{\infty} \Pi_{p,n} A^*_n e^{i\mu_n b} Y_n \quad \text{on } \Gamma_*. \tag{2.40}$$

If $z$ is expanded as the series, $z(x,y) = \sum_{n=0}^{\infty}(A_n e^{i\mu_n x} + B_n e^{-i\mu_n x})Y_n(y)$, then (2.40) yields the system of linear equations

$$\begin{aligned} Q_{p,n}A_n + \frac{1}{Q_{p,n}} B_n &= -Q_{p,n}A^E_n, \\ \frac{1}{Q_{p,n}} A_n + Q_{p,n}B_n &= -Q_{p,n}A^W_n, \end{aligned}$$

where $Q_{p,n} = \Pi_{p,n} e^{i\mu_n b}$. Since $u = z + u_{ex}$, solving the above equations for $A_n$ and $B_n$ leads to

$$u|_{\Gamma_E} = \sum_{n=0}^{\infty} \frac{(1-\Pi_{p,n}^2)e^{i\mu_n b}}{1-Q_{p,n}^4}\big(A_n^E - Q_{p,n}^2 A_n^W\big)Y_n \tag{2.41}$$

and

$$\left.\frac{\partial u}{\partial x}\right|_{\Gamma_E} = \sum_{n=0}^{\infty} i\mu_n \frac{e^{2i\mu_n b} + Q_{p,n}^2}{(1-Q_{p,n}^4)e^{i\mu_n b}}\big(A_n^E - Q_{p,n}^2 A_n^W\big)Y_n. \tag{2.42}$$

Therefore, by using the definition of the DtN operator (2.34), (2.41) and (2.42), we obtain that

$$\left\| T^E(u) - \frac{\partial u}{\partial x}\right\|_{H^{-1/2}(\Gamma_E)}^2 = \left\| \sum_{n=0}^{\infty} i\mu_n \frac{-\Pi_{p,n}^2}{1-Q_{p,n}^4}\big(e^{i\mu_n b}A_n^E - Q_{p,n}^2 e^{i\mu_n b}A_n^W\big)Y_n\right\|_{H^{-1/2}(\Gamma_E)}^2.$$

Now, we note that there exists $N > 0$ such that

$$\left\| \sum_{n=N+1}^{\infty} i\mu_n A_n^* Y_n\right\|_{H^{-1/2}(\Gamma_*)} \leqslant \varepsilon \|u_{ex}\|_{H^{1/2}(\Gamma_*)},$$

and define $M(\varepsilon, u_{ex}) = \max|(a_j + i\mu_n)/(a_j - i\mu_n)| < 1$, where the maximum is taken over $0 \leqslant j \leqslant p, 0 \leqslant n \leqslant N$. Since $|\Pi_{p,n}| < 1$ and $|Q_{p,n}| < C_Q < 1$ for all $n \geqslant 0$ and $p \geqslant 0$ with a positive constant $C_Q$, a triangle inequality and trace theorem shows that

$$\begin{aligned}
\left\| T^E(u) - \frac{\partial u}{\partial x}\right\|_{H^{-1/2}(\Gamma_E)}^2 &= CM^{4(p+1)}\left\| \sum_{n=0}^{N} i\mu_n\big(e^{i\mu_n b}A_n^E - Q_{p,n}^2 e^{i\mu_n b}A_n^W\big)Y_n\right\|_{H^{-1/2}(\Gamma_E)}^2 \\
&\quad + \left\| \sum_{n=N+1}^{\infty} i\mu_n\big(e^{i\mu_n b}A_n^E - Q_{p,n}^2 e^{i\mu_n b}A_n^W\big)Y_n\right\|_{H^{-1/2}(\Gamma_E)}^2 \\
&\leqslant C\big(M^{4(p+1)} + \varepsilon^2\big)\big(\|u_{ex}\|_{H^{1/2}(\Gamma_E)}^2 + \|u_{ex}\|_{H^{1/2}(\Gamma_W)}^2\big) \\
&\leqslant C\big(M^{4(p+1)} + \varepsilon^2\big)\|u_{ex}\|_{H^1(\Omega_b)}^2.
\end{aligned} \tag{2.43}$$

Finally, combining (2.36), (2.43) and the analogous inequality on $\Gamma_W$ yields the desired inequality (2.33).

## 3. Complete radiation boundary conditions for the convected Helmholtz equation in waveguides

In this section, we consider a time-harmonic acoustic wave propagation problem in $\Omega_\infty$ carrying a uniform mean flow. In this case, the governing equation is the convected Helmholtz equation

$$\big(1-M^2\big)\frac{\partial^2 u}{\partial x^2} + \frac{\partial^2 u}{\partial y^2} + 2ikM\frac{\partial u}{\partial x} + k^2 u = f \quad \text{in } \Omega_\infty. \tag{3.1}$$

Here $M$ is the Mach number and we consider the subsonic case, $0 < M < 1$. Again, we assume that a source function $f$ is supported in $|x| < L$ for a positive constant $L$ and the North and South boundaries $\widetilde{\Gamma}_T$ of $\Omega_\infty$ are sound-hard:

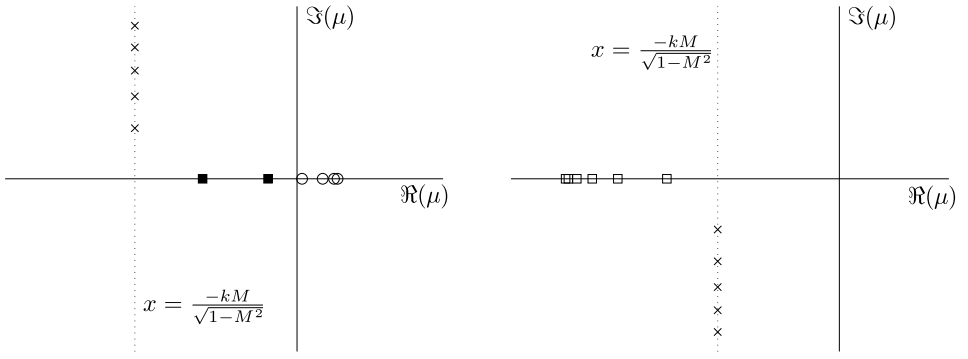
$$\frac{\partial u}{\partial n} = 0 \quad \text{on } \widetilde{\Gamma}_N \cup \widetilde{\Gamma}_S. \tag{3.2}$$

Before proceeding with development of complete radiation boundary conditions for the convected Helmholtz equation, outgoing radiating solutions to the model problem (3.1) will be characterized by using Fourier modes analysis. It is known that the convected Helmholtz equation may support waves which have a mismatch between the directions of phase velocity and group velocity, that is, there may be waves that move to the left with respect to phase velocity but go out to the right with group velocity. In this case, a physically meaningful solution radiating to the right (left, respectively) is defined by one that is represented by a superposition of modes with positive (negative, respectively) group velocity and evanescent modes. This characterization of outgoing radiating solutions is analyzed in [2], and we provide a brief description on it. For $|x| > L$, the coefficient $X_n(x)$ of the modal basis function $Y_n$ is given by

$$X_n(x) = A_n e^{i\mu_n x} + B_n e^{-i\mu_n x},$$

where $\mu_n$ is a solution to the equation

$$\big(1-M^2\big)\mu_n^2 + 2kM\mu_n + \lambda_n^2 - k^2 = 0, \tag{3.3}$$




(a) Plot of $\mu_n^+$ (b) Plot of $\mu_n^-$

**Fig. 3.** Plots of $\mu_n^\pm$ obtained with $W = 10$, $M = 0.8$, $k = 1$. (a) The modes associated with ∘ are propagating to the right with respect to *phase* velocity, the modes associated with ■ are propagating to the left with respect to *phase* velocity. In contrast, both modes corresponding to ∘ and ■ are propagating to the right with respect to *group* velocity. The modes with × are evanescent to the right. (b) The modes associated with □ are propagating to the left with respect to both of *phase* and *group* velocities and the modes with × are evanescent to the left.

i.e., denoting $\eta = kM/(1-M^2)$ and $\beta_n = \sqrt{k^2 - (1-M^2)\lambda_n^2}/\sqrt{1-M^2}$

$$\mu_n^\pm = \frac{-kM \pm \sqrt{k^2 - (1-M^2)\lambda_n^2}}{1-M^2} = -\eta \pm \frac{\beta_n}{\sqrt{1-M^2}}. \tag{3.4}$$

To understand all wave motions that can occur in a uniform mean flow in the waveguide, we examine the real and imaginary parts of $\mu_n^\pm$ and see that $\mu_n^+$ is

$$\begin{cases} \text{a real number} \geqslant 0 & \text{for } 0 \leqslant n \leqslant kW/\pi, \\ \text{a real number} < 0 & \text{for } kW/\pi < n < kW/(\alpha\pi), \\ \text{a complex number with } \Im(\mu_n^+) > 0 & \text{for } kW/(\alpha\pi) < n \end{cases}$$

and $\mu_n^-$ is

$$\begin{cases} \text{a real number} < 0 & \text{for } 0 \leqslant n < kW/(\alpha\pi), \\ \text{a complex number with } \Im(\mu_n^-) < 0 & \text{for } kW/(\alpha\pi) < n, \end{cases}$$

where $\alpha = \sqrt{1-M^2}$ (see Fig. 3). Here we assume that there is no cutoff mode, i.e., $n \neq kW/(\alpha\pi)$ for the well-posedness of the problem. Fig. 3 provides an information on the distribution of axial wavenumbers in case of $W = 10$, $M = 0.8$ and $k = 1$. In (a) of Fig. 3, the modes (downstream modes) associated with ∘ for $0 \leqslant n < kW/\pi$ are propagating to the right with respect to phase velocity, $\omega/\mu_n^+$, and the modes (upstream modes) associated with ■ for $kW/\pi < n < kW/(\alpha\pi)$ are propagating to the left with respect to phase velocity. The modes with × for $kW/(\alpha\pi) < n$ are evanescent to the right. In (b) of Fig. 3, the modes associated with □ for $0 \leqslant n < kW/(\alpha\pi)$ are propagating to the left with respect to of phase velocity, $\omega/\mu_n^-$, and the modes with × for $kW/(\alpha\pi) < n$ decay exponentially to the left.

On the other hand, for $n$ with $0 \leqslant n < kW/(\alpha\pi)$, from the relation (3.4) between the axial wavenumber $\mu_n$ and the angular frequency $\omega = c_0 k$, we can compute the group velocity and observe that

$$\frac{\partial\omega}{\partial\mu_n^\pm} = \pm\frac{c_0(1-M^2)\sqrt{k^2 - \lambda_n^2(1-M^2)}}{k \mp M\sqrt{k^2 - \lambda_n^2(1-M^2)}} \gtrless 0.$$

Therefore, the modes associated with $\mu_n^+$ ($\mu_n^-$, respectively) represent outgoing waves to the right (to the left, respectively) with respect to group velocity and hence the radiating solutions need to be represented by the following series

$$u(x,y) = \sum_{n=0}^{\infty} A_n^+ e^{i\mu_n^+ x} Y_n(y) \quad \text{for } x > L \tag{3.5}$$

and

$$u(x,y) = \sum_{n=0}^{\infty} A_n^- e^{i\mu_n^- x} Y_n(y) \quad \text{for } x < -L. \tag{3.6}$$

If there exists $n$ such that $kW/\pi < n < kW/(\alpha\pi)$, then an axial wavenumber $\mu_n^+$ is real and negative, in which case a solution may include upstream modes. If standard CRBCs analyzed in Section 2 were imposed on the boundary $\Gamma_E$, the reflection coefficient of the upstream modes,

$$R = -\prod_{j=0}^{p}\left(\frac{a_j + i\mu_n^+}{a_j - i\mu_n^+}\right)^2,$$

would grow exponentially as $p$ approaches infinity. Therefore, in numerical simulations of wave propagations involving upstream modes, a special care needs to be taken on artificial boundaries. To handle this kind of modes correctly on artificial boundaries, we modify CRBCs by noticing the convected Helmholtz equation is related with a Helmholtz equation via Prandtl–Glauert transformation.

### 3.1. Modification of CRBCs via Prandtl–Glauert transformation

In order to introduce complete radiation boundary conditions for the convected Helmholtz equation, we start by applying a Prandtl–Glauert transformation to convert the convected Helmholtz equation (3.1) to the Helmholtz equation. Using the change of variables

$$(\tilde{x}, \tilde{y}) = (x/\alpha, y),$$

the transformed functions

$$\tilde{u}(\tilde{x}, \tilde{y}) = e^{i\eta x}u(x, y) \quad \text{and} \quad \tilde{f}(\tilde{x}, \tilde{y}) = e^{i\eta x}f(x, y)$$

satisfy the Helmholtz equation with wavenumber $\tilde{k} = k/\alpha$,

$$\widetilde{\Delta}\tilde{u} + \tilde{k}^2\tilde{u} \equiv \frac{\partial^2\tilde{u}}{\partial\tilde{x}^2} + \frac{\partial^2\tilde{u}}{\partial\tilde{y}^2} + \tilde{k}^2\tilde{u} = \tilde{f} \quad \text{in } \Omega_\infty. \tag{3.7}$$

It is easy to show that the radiating solutions to the Helmholtz equation with the series representations

$$\tilde{u}(\tilde{x}, \tilde{y}) = \sum_{n=0}^{\infty} A_n^+ e^{i\beta_n\tilde{x}}Y_n(\tilde{y}) \quad \text{for } \tilde{x} > \frac{L}{\alpha}$$

and

$$\tilde{u}(\tilde{x}, \tilde{y}) = \sum_{n=0}^{\infty} A_n^- e^{-i\beta_n\tilde{x}}Y_n(\tilde{y}) \quad \text{for } \tilde{x} < -\frac{L}{\alpha}$$

correspond to the radiating solutions with the series expansions (3.5) and (3.6) to the convected Helmholtz equation via the Prandtl–Glauert transformation.

We truncate the infinite waveguide $\Omega_\infty$ to a bounded region $\widetilde{\Omega}_b$, whose vertical absorbing boundaries $\widetilde{\Gamma}_E$ and $\widetilde{\Gamma}_W$ are located at $\tilde{x} = b/\alpha$ and $\tilde{x} = -b/\alpha$ respectively for $b > L$, and impose complete radiation boundary conditions on the artificial boundaries. Let $\widetilde{I}_E = (L/\alpha, b/\alpha)$ and $\widetilde{I}_W = (-b/\alpha, -L/\alpha)$. As seen in Section 2, the boundary conditions on $\widetilde{\Gamma}_*$ (with $*$ representing $E$ or $W$) are given by auxiliary functions $\tilde{\phi}_j^*$ satisfying the Helmholtz equation

$$\widetilde{\Delta}\tilde{\phi}_j^* + \tilde{k}^2\tilde{\phi}_j^* = 0 \quad \text{in } \widetilde{I}_* \times I_y \tag{3.8}$$

with $\partial\tilde{\phi}_j^*/\partial n = 0$ on $\widetilde{I}_* \times \partial I_y$ and the recursive formulas in $\widetilde{I}_* \times I_y$

$$\begin{aligned} &\tilde{\phi}_0^* = \tilde{u}, \\ &\left(\pm\frac{\partial}{\partial\tilde{x}} + \tilde{a}_j\right)\tilde{\phi}_j^* = \left(\mp\frac{\partial}{\partial\tilde{x}} + \tilde{a}_j\right)\tilde{\phi}_{j+1}^* \end{aligned} \tag{3.9}$$

for $j = 0, \ldots, p$ with $\tilde{a}_j = \alpha a_j$. This recursion is terminated by

$$\tilde{\phi}_{p+1}^* = 0 \quad \text{on } \tilde{x} = \pm\frac{b}{\alpha}.$$

Here the auxiliary functions for the boundary conditions on $\widetilde{\Gamma}_E$ correspond to the upper sign and those for the boundary conditions on $\widetilde{\Gamma}_W$ correspond to the lower sign.

Now, in order to derive absorbing boundary conditions for waves in the uniform flow, we shall revert these boundary conditions back to the convected problem by using the Prandtl–Glauert transformation. We introduce

$$\phi_j^*(x, y) = e^{-i\eta x}\tilde{\phi}_j^*(\tilde{x}, \tilde{y}),$$

and substitute $\phi_j^*$ into (3.8) and (3.9) to show that $\phi_j^*$ are functions satisfying the convected Helmholtz equation

$$\left(\frac{\partial}{\partial x}+i\eta\right)^2\phi_j^*+\frac{1}{\alpha^2}\frac{\partial^2}{\partial y^2}\phi_j^*+\frac{k^2}{\alpha^4}\phi_j^*=0 \quad \text{in } I_*\times I_y \tag{3.10}$$

with $\partial\phi_j^*/\partial n=0$ on $I_*\times\partial I_y$ and the recursions

$$\begin{aligned}&\phi_0^*=u,\\ &\left(\pm\left(\frac{\partial}{\partial x}+i\eta\right)+a_j\right)\phi_j^*=\left(\mp\left(\frac{\partial}{\partial x}+i\eta\right)+a_j\right)\phi_{j+1}^*\end{aligned} \tag{3.11}$$

with the terminal condition

$$\phi_{p+1}^*=0 \quad \text{on } x=\pm b.$$

Next, we eliminate the $x$-derivatives from the recursive formulas (3.11) to derive a practical boundary conditions suitable for numerical computations. The same algebraic computation as done with CRBCs for the Helmholtz equation leads to the boundary conditions

$$\left(\frac{\partial}{\partial x}+i\eta\right)u\boldsymbol{e}_0=\frac{1}{2}\left(\frac{1}{\alpha^2}L\frac{\partial^2\Phi^E}{\partial y^2}+\left(\frac{k^2}{\alpha^4}L-M\right)\Phi^E\right) \quad \text{on } \Gamma_E \tag{3.12}$$

and

$$\left(\frac{\partial}{\partial x}+i\eta\right)u\boldsymbol{e}_0=\frac{-1}{2}\left(\frac{1}{\alpha^2}L\frac{\partial^2\Phi^W}{\partial y^2}+\left(\frac{k^2}{\alpha^4}L-M\right)\Phi^W\right) \quad \text{on } \Gamma_W \tag{3.13}$$

with

$$\frac{\partial\Phi^E}{\partial n}=0 \quad \text{at } \partial\Gamma_E \quad \text{and} \quad \frac{\partial\Phi^W}{\partial n}=0 \quad \text{at } \partial\Gamma_W.$$

**Remark 3.1.** According to (3.11), the CRBCs for the convected Helmholtz equation is obtained by the translation by $i\eta$ followed by the standard CRBCs. It is not surprising that the new PML proposed in [2] for the convected Helmholtz equation is in fact standard PML supplemented with the translation by $i\eta$ due to the relation between the convected Helmholtz equation and the Helmholtz equation by the Prandtl–Glauert transformation.

### 3.2. Well-posedness and convergence

The model problem (3.1) truncated to the finite domain $\Omega_b$ can be completed by the CRBCs (3.12) and (3.13) and be written in a weak formulation to seek for $(u,\Phi^E,\Phi^W)\in\boldsymbol{H}$ satisfying

$$A_c\big((u,\Phi^E,\Phi^W),(\xi,\Psi^E,\Psi^W)\big)=(2f,\xi)_{\Omega_b} \quad \text{for all } (\xi,\Psi^E,\Psi^W)\in\boldsymbol{H}, \tag{3.14}$$

where

$$\begin{aligned}&A_c\big((u,\Phi^E,\Phi^E),(\xi,\Psi^E,\Psi^W)\big)\\ &\quad=2\alpha^2\left(\left(\frac{\partial}{\partial x}+i\eta\right)u,\left(\frac{\partial}{\partial x}+i\eta\right)\xi\right)_{\Omega_b}+2\left(\frac{\partial u}{\partial y},\frac{\partial\xi}{\partial y}\right)_{\Omega_b}-2\frac{k^2}{\alpha^2}(u,\xi)_{\Omega_b}\\ &\qquad+\left(L\frac{\mathrm{d}\Phi^E}{\mathrm{d}y},\frac{\mathrm{d}\Psi^E}{\mathrm{d}y}\right)_{\Gamma_E}+\left(\left(-\frac{k^2}{\alpha^2}L+\alpha^2M\right)\Phi^E,\Psi^E\right)_{\Gamma_E}\\ &\qquad+\left(L\frac{\mathrm{d}\Phi^W}{\mathrm{d}y},\frac{\mathrm{d}\Psi^W}{\mathrm{d}y}\right)_{\Gamma_E}+\left(\left(-\frac{k^2}{\alpha^2}L+\alpha^2M\right)\Phi^E,\Psi^W\right)_{\Gamma_W}.\end{aligned}$$

Now, the essentially same ideas used in Lemma 2.1 and Lemma 2.4 (uniqueness of solutions and compact perturbation arguments) can be carried out to prove that the problem (3.14) is well-posed.

**Theorem 3.2.** *For $f\in L^2(\Omega_b)$ supported in $|x|<L$, the problem (3.14) has a unique solution $(u,\Phi^E,\Phi^W)\in\boldsymbol{H}$ such that*

$$\|(u,\Phi^E,\Phi^W)\|_{\boldsymbol{H}}\leqslant C\|f\|_{L^2(\Omega_b)}.$$

Finally, the Prandtl–Glauert transformation allows to prove the convergence of approximate solutions satisfying CRBCs (3.12) and (3.13).

**Theorem 3.3.** *Suppose that $u_{ex}$ is the radiating solution to the problem (3.1) for $f \in L^2(\Omega_b)$ supported in $|x| < L$. If $(u, \Phi^E, \Phi^W) \in \boldsymbol{H}$ is an approximate solution to the problem (3.14), then for any $\varepsilon > 0$ there exists a positive constant $M(\varepsilon, u_{ex}) > 0$ such that*

$$\|u - u_{ex}\|_{H^1(\Omega_b)} \leqslant C\big(M^{2(p+1)} + \varepsilon\big)\|u_{ex}\|_{H^1(\Omega_b)}$$

*with $C$ independent of $\varepsilon$, $u$, $u_{ex}$ and $p$.*

**Proof.** A straightforward computation shows that for any $v \in H^1(\Omega_b)$, the function $\tilde{v}(\tilde{x}, \tilde{y}) = e^{i\eta x}v(x, y)$ transformed by the Prandtl–Glauert transformation satisfies

$$C_1\|\tilde{v}\|_{H^1(\widetilde{\Omega}_b)} < \|v\|_{H^1(\Omega_b)} \leqslant C_2\|\tilde{v}\|_{H^1(\widetilde{\Omega}_b)}.$$

Then, by using the boundedness of the Prandtl–Glauert transformation and Theorem 2.6

$$\begin{aligned}\|u - u_{ex}\|_{H^1(\Omega_b)} &\leqslant C\|\tilde{u} - \tilde{u}_{ex}\|_{H^1(\widetilde{\Omega}_b)} \\ &\leqslant C\big(M^{2(p+1)} + \varepsilon\big)\|\tilde{u}_{ex}\|_{H^1(\widetilde{\Omega}_b)} \\ &= C\big(M^{2(p+1)} + \varepsilon\big)\|u_{ex}\|_{H^1(\Omega)},\end{aligned}$$

which completes the proof. □

## 4. Numerical experiments

This section of numerical simulations is devoted to confirming the theories on well-posedness and convergence. The first example is intended to demonstrate convergence of approximate solutions satisfying CRBCs of order $p$ as $p$ increases. We consider the acoustic waveguide problem with a Dirichlet boundary condition imposed on $\Gamma_W$ and CRBCs on $\Gamma_E$:

$$\big(1 - M^2\big)\frac{\partial^2 u}{\partial x^2} + 2ikM\frac{\partial u}{\partial x} + \frac{\partial^2 u}{\partial y^2} + k^2 u = 0 \quad \text{in } \Omega_b$$

with $u = g$ on $\Gamma_W$, where wavenumber and Mach number are chosen to be $k = 4$ and $M = 0.8$ and the computational domain $\Omega_b$ is set to be $\Omega_b = (0, 2) \times (0, 5)$. In this case, modes associated with $0 \leqslant n \leqslant 6$ are propagating downstream, however modes with $7 \leqslant n \leqslant 10$ are propagating upstream and hence they have a direction mismatch of phase and group velocity. To demonstrate the efficiency of CRBCs on $\Gamma_E$ in each case, two different boundary data for $g$ are considered. The first one is a boundary function $g$ for which the exact solution $u_{ex}$ is given by

$$u_{ex}(x, y) = \sum_{n=0}^{6} \frac{1}{2^n} e^{i\mu_n^+ x} Y_n(y),$$

which includes only downstream propagating modes. The other case involves the exact solution given by

$$u_{ex}(x, y) = \sum_{n=7}^{10} \frac{1}{2^{n-7}} e^{i\mu_n^+ x} Y_n(y)$$

including upstream propagating modes. The numerical simulations are conducted with two different sets of damping parameters defined as in (2.7) with $\theta_j = \frac{(j+1)\pi}{2(p+2)}$ for $j = 0, \ldots, p$ and (2.10) with $c_j = 1$. When (2.10) is employed, we do not use $\sigma_j$ since we consider only the case when the analytic solution excludes evanescent modes. All computational results are obtained by using the finite element library deal.II [1] with bilinear finite elements. The convergence behavior is observed by estimating the relative $L^2$ errors as a function of $p$:

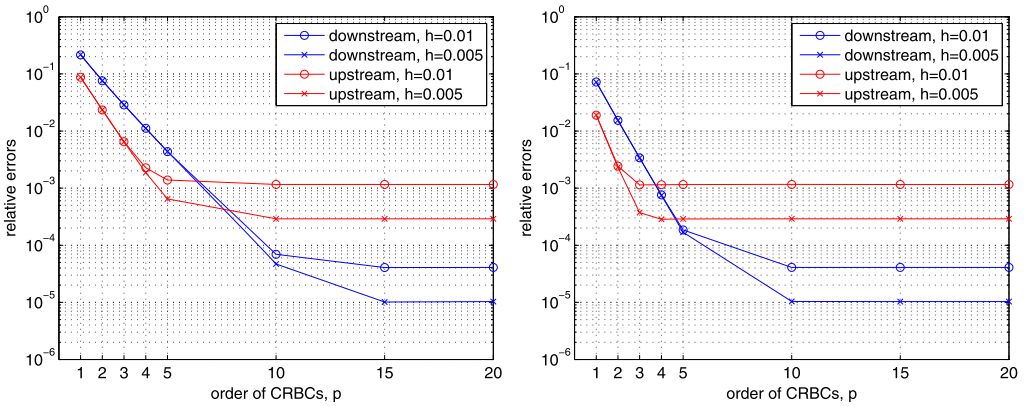
$$\frac{\|u - u_{ex}\|_{L^2(\Omega_b)}}{\|u_{ex}\|_{L^2(\Omega_b)}}.$$

From the plots in Fig. 4, the performances of CRBCs with two different type of damping parameters appear to have quite similar effectiveness. They indicate the relative $L^2$ errors get smaller as the order $p$ of CRBCs gets larger until the mesh size error dominates.

As a matter of fact, the optimal choice of the damping parameters $a_j$ in this specific example is determined by the axial wavenumber $\mu_n^+$, i.e., $a_j = -\beta_j/\sqrt{1 - M^2}$, since the differential operators involving CRBCs eliminate the corresponding propagating modes. The relative $L^2$ errors for this choice of $a_j$ are reported in Table 1. It is observed that the errors in Fig. 4 are not smaller than the errors in Table 1 even though $p$ is large with the mesh size fixed. Fig. 5 and Fig. 6 provide real parts of the approximate downstream and upstream solutions satisfying CRBCs of order $p = 1, 2, 5$ and 20 and the exact solution.

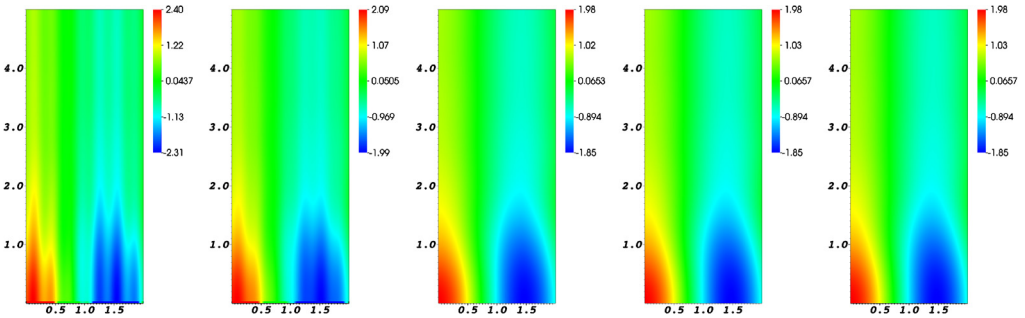
**Table 1**
Errors obtained by CRBCs with the optimal parameters.

| | $p$ | $h = 0.01$ | $h = 0.005$ |
|---|---|---|---|
| downstream | 6 | 4.07995e-05 | 1.03133e-05 |
| upstream | 3 | 1.15758e-03 | 2.89665e-04 |



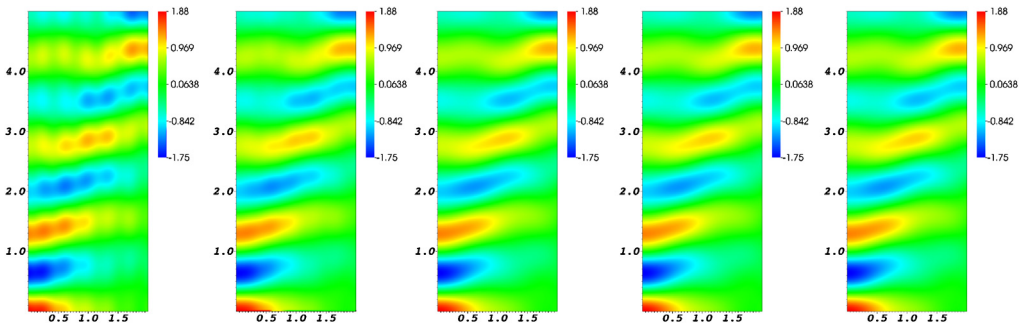

(a) $a_j = \sigma_j - ikc_j$ (b) $a_j = -ikc_j$

**Fig. 4.** Error plots as a function of order $p$.



(a) $p = 1$ (b) $p = 2$ (c) $p = 5$ (d) $p = 20$ (e) $u_{ex}$

**Fig. 5.** Real parts of solutions including downstream propagating modes.

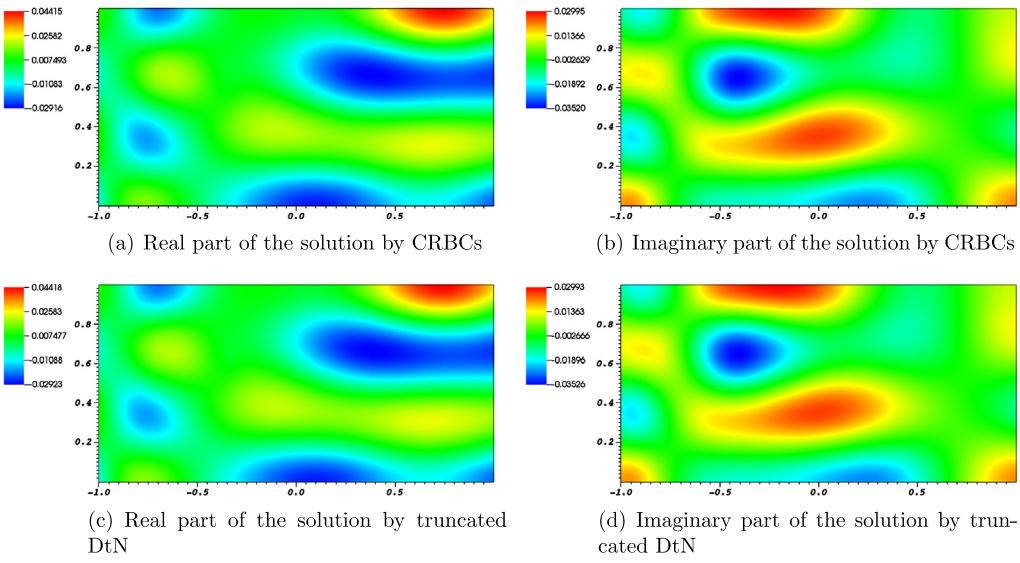


(a) $p = 1$ (b) $p = 2$ (c) $p = 5$ (d) $p = 20$ (e) $u_{ex}$

**Fig. 6.** Real parts of solutions including upstream propagating modes.

In the second example, we are concerned with a source problem (3.1) in $\Omega_b = (-1, 1) \times (0, 1)$ with $k = 9$, $M = 0.4$ and the wave source $f$ defined by

$$f(x, y) = \begin{cases} 1 & \text{if } (x + 0.5)^2 + (y - 0.6)^2 < 0.04, \\ 0 & \text{elsewhere.} \end{cases}$$




(a) Real part of the solution by CRBCs

(b) Imaginary part of the solution by CRBCs

(c) Real part of the solution by truncated DtN

(d) Imaginary part of the solution by truncated DtN

**Fig. 7.** Approximate solutions to the source problem obtained by CRBCs or DtN.

In this case, there are 3 downstream and 1 upstream propagating modes. Evanescent modes may be involved but they decay fast near the absorbing boundaries. Therefore, CRBCs are set up to control only 4 propagating modes, i.e., we take the damping parameters $a_j$ in a way that the differential operators of CRBCs with $p = 3$ remove all the propagating modes. The results of the computation are given in Fig. 7. The computation was done with the mesh size $h = 0.01$. For a reference solution to the problem, Fig. 7 also provides approximate solutions obtained by applying truncated Dirichlet-to-Neumann (DtN) boundary conditions to the absorbing boundaries. Here the DtN boundary conditions are truncated so that the approximate DtN operator includes only the 4 propagating modes. From Fig. 7, it can be seen that the approximate solutions obtained by two different methods are qualitatively the same. When the order $p$ of CRBCs and the number of terms of truncated DtN operator increases, no improvement is observed.

## Acknowledgments

This research was supported by Basic Science Research Program through the National Research Foundation of Korea (NRF) funded by the Ministry of Education, Science and Technology (2012R1A1A1002121).

## References

[1] W. Bangerth, R. Hartmann, G. Kanschat, deal.II — a general-purpose object-oriented finite element library, ACM Trans. Math. Software 33 (4) (2007), Art. 24, 27.
[2] E. Bécache, A.-S. Bonnet-Ben Dhia, G. Legendre, Perfectly matched layers for the convected Helmholtz equation, SIAM J. Numer. Anal. 42 (1) (2004) 409–433.
[3] A. Bendali, P. Guillaume, Non-reflecting boundary conditions for waveguides, Math. Comp. 68 (225) (1999) 123–144.
[4] J.-P. Berenger, A perfectly matched layer for the absorption of electromagnetic waves, J. Comput. Phys. 114 (2) (1994) 185–200.
[5] J.-P. Berenger, Three-dimensional perfectly matched layer for the absorption of electromagnetic waves, J. Comput. Phys. 127 (2) (1996) 363–379.
[6] D. Givoli, Nonreflecting boundary conditions, J. Comput. Phys. 94 (1) (1991) 1–29.
[7] D. Givoli, B. Neta, High-order non-reflecting boundary scheme for time-dependent waves, J. Comput. Phys. 186 (1) (2003) 24–46.
[8] D. Givoli, I. Patlashenko, Dirichlet-to-Neumann boundary condition for time-dependent dispersive waves in three-dimensional guides, J. Comput. Phys. 199 (1) (2004) 339–354.
[9] C.I. Goldstein, A finite element method for solving Helmholtz type equations in waveguides and other unbounded domains, Math. Comp. 39 (160) (1982) 309–324.
[10] T. Hagstrom, Radiation boundary conditions for the numerical simulation of waves, Acta Numer. 8 (1999) 47–106.
[11] T. Hagstrom, E. Bécache, D. Givoli, K. Stein, Complete radiation boundary conditions for convective waves, Commun. Comput. Phys. 11 (2) (2012) 610–628.
[12] T. Hagstrom, A. Mar-Or, D. Givoli, High-order local absorbing conditions for the wave equation: extensions and improvements, J. Comput. Phys. 227 (6) (2008) 3322–3357.
[13] T. Hagstrom, T. Warburton, A new auxiliary variable formulation of high-order local radiation boundary conditions: corner compatibility conditions and extensions to first-order systems, Wave Motion 39 (4) (2004) 327–338, new computational methods for wave propagation.
[14] T. Hagstrom, T. Warburton, Complete radiation boundary conditions: minimizing the long time error growth of local methods, SIAM J. Numer. Anal. 47 (5) (2009) 3678–3704.
[15] T. Hagstrom, T. Warburton, D. Givoli, Radiation boundary conditions for time-dependent waves based on complete plane wave expansions, J. Comput. Appl. Math. 234 (6) (2010) 1988–1995.
[16] I. Harari, I. Patlashenko, D. Givoli, Dirichlet-to-Neumann maps for unbounded wave guides, J. Comput. Phys. 143 (1) (1998) 200–223.

[17] R.L. Higdon, Absorbing boundary conditions for difference approximations to the multidimensional wave equation, Math. Comp. 47 (176) (1986) 437–459.
[18] R.L. Higdon, Numerical absorbing boundary conditions for the wave equation, Math. Comp. 49 (179) (1987) 65–90.
[19] S. Kim, T. Hagstrom, Complete radiation boundary conditions for the Helmholtz equation I: waveguides, submitted for publication.
[20] S.V. Tsynkov, Numerical solution of problems on unbounded domains. A review, Appl. Numer. Math. 27 (4) (1998) 465–532, absorbing boundary conditions.